

# Does the Higher Metal Oxidation State Necessarily Imply the Higher Reactivity toward H-Atom Transfer? A Computational Study of C-H Bond Oxidation by High-Valent Iron-Oxo and -Nitrido Complexes

Caiyun Geng, Shengfa Ye,\* Frank Neese\*

Max-Planck Institute for Chemical Energy Conversion

Stiftstr. 34-36

D-45470 Mülheim an der Ruhr

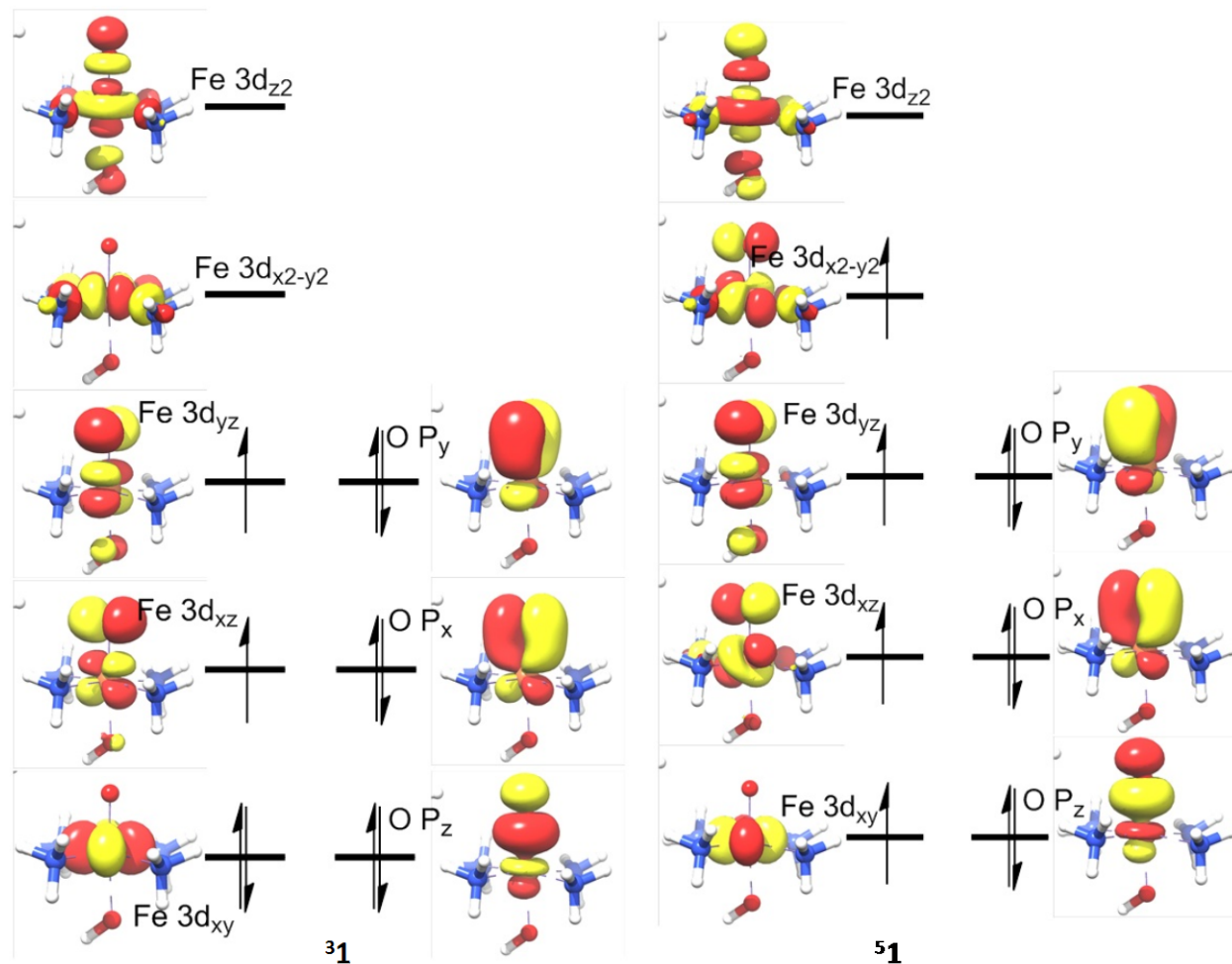
Germany

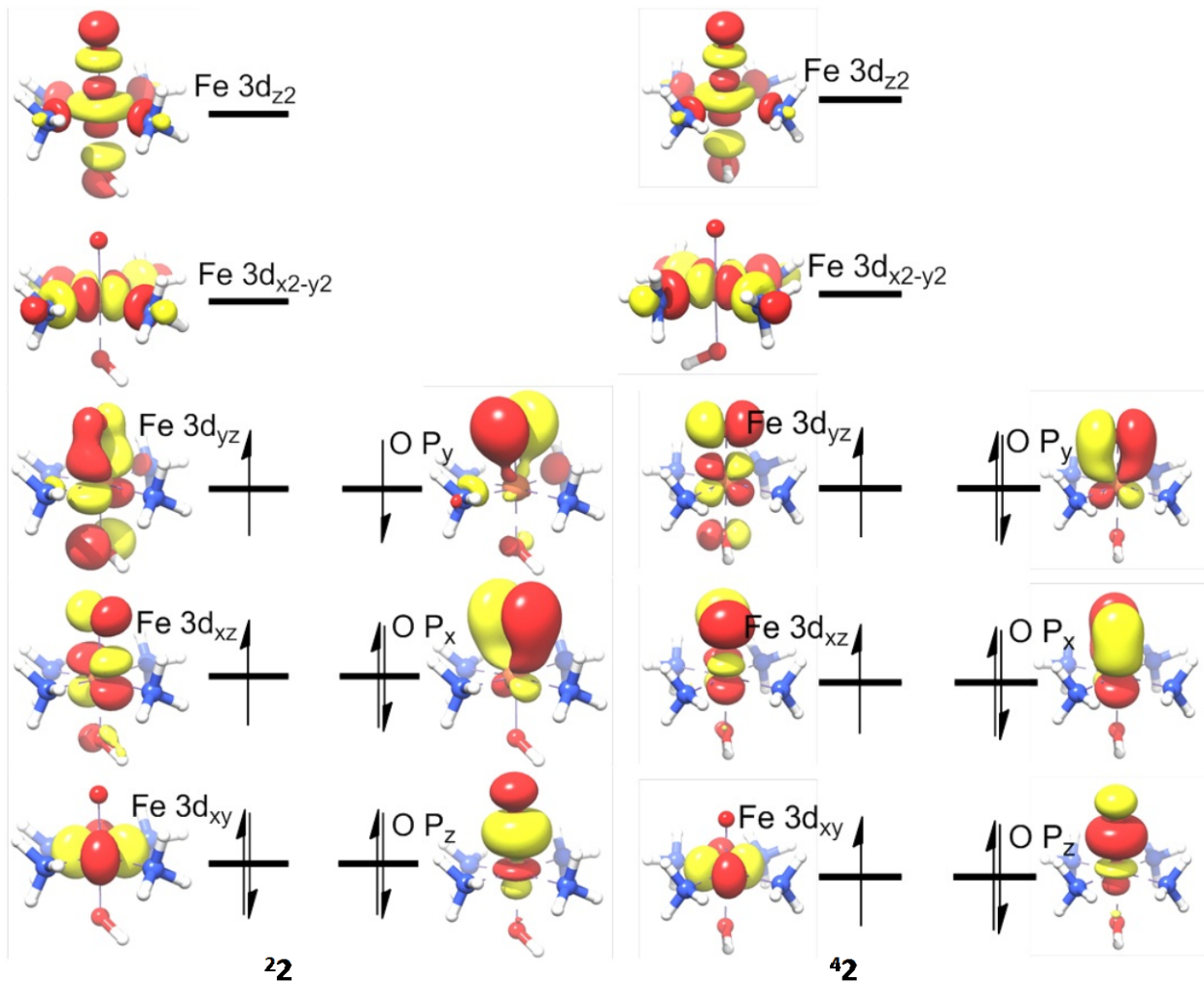
E-Mail: shengfa.ye@cec.mpg.de, frank.neese@cec.mpg.de

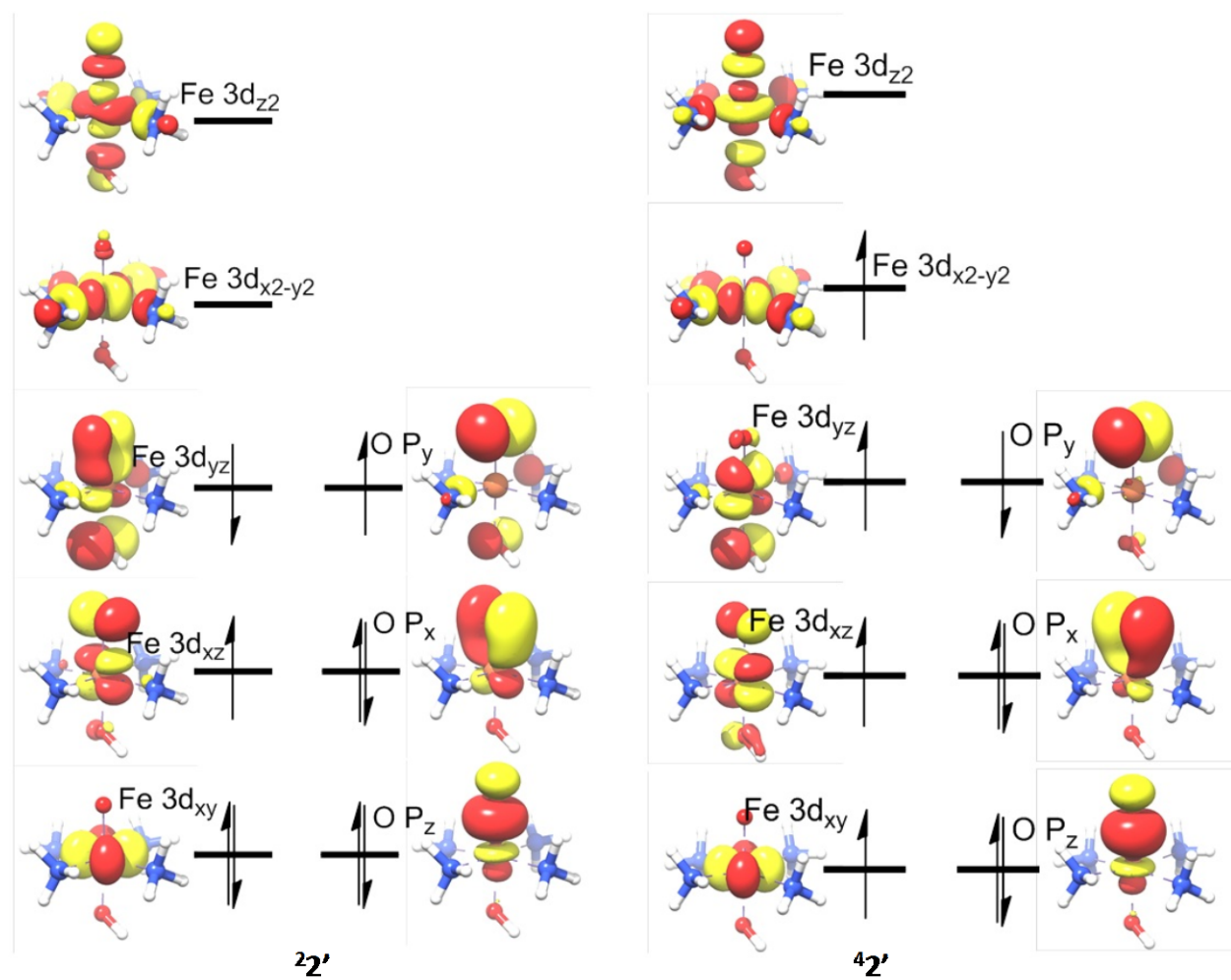
Table S1 collects the selected geometric parameters structures and Figure S1 and S2 present all the schematic MO diagrams calculated by B3LYP and BP86 functionals.

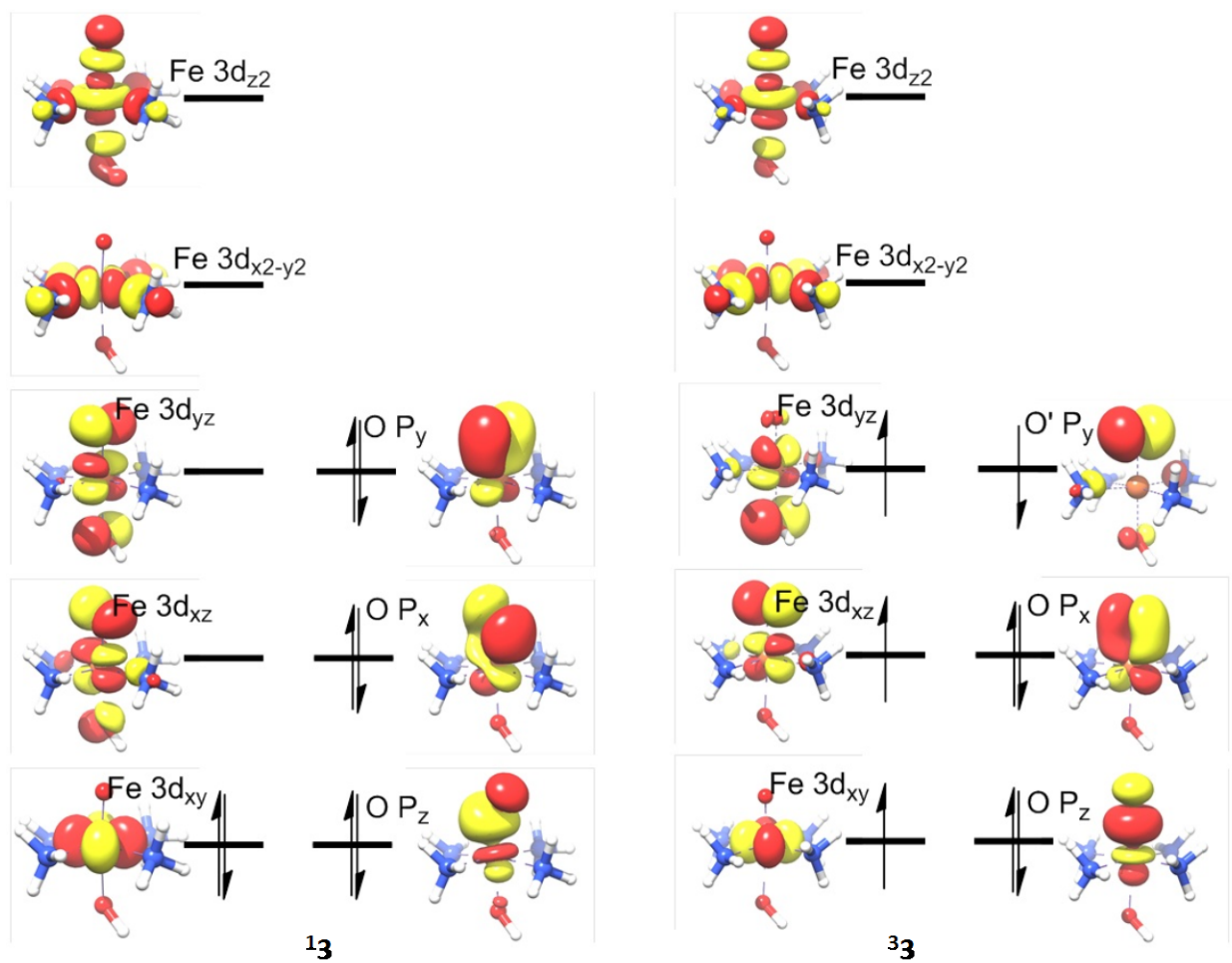
Table S1, Calculated Energies and Selected Geometric Parameters for the “Superoxidized” Iron–Oxo and –Nitrido Complexes predicted by B3LYP and BP86 calculations (Energy in kcal/mol and Bond Distances in Angstroms).

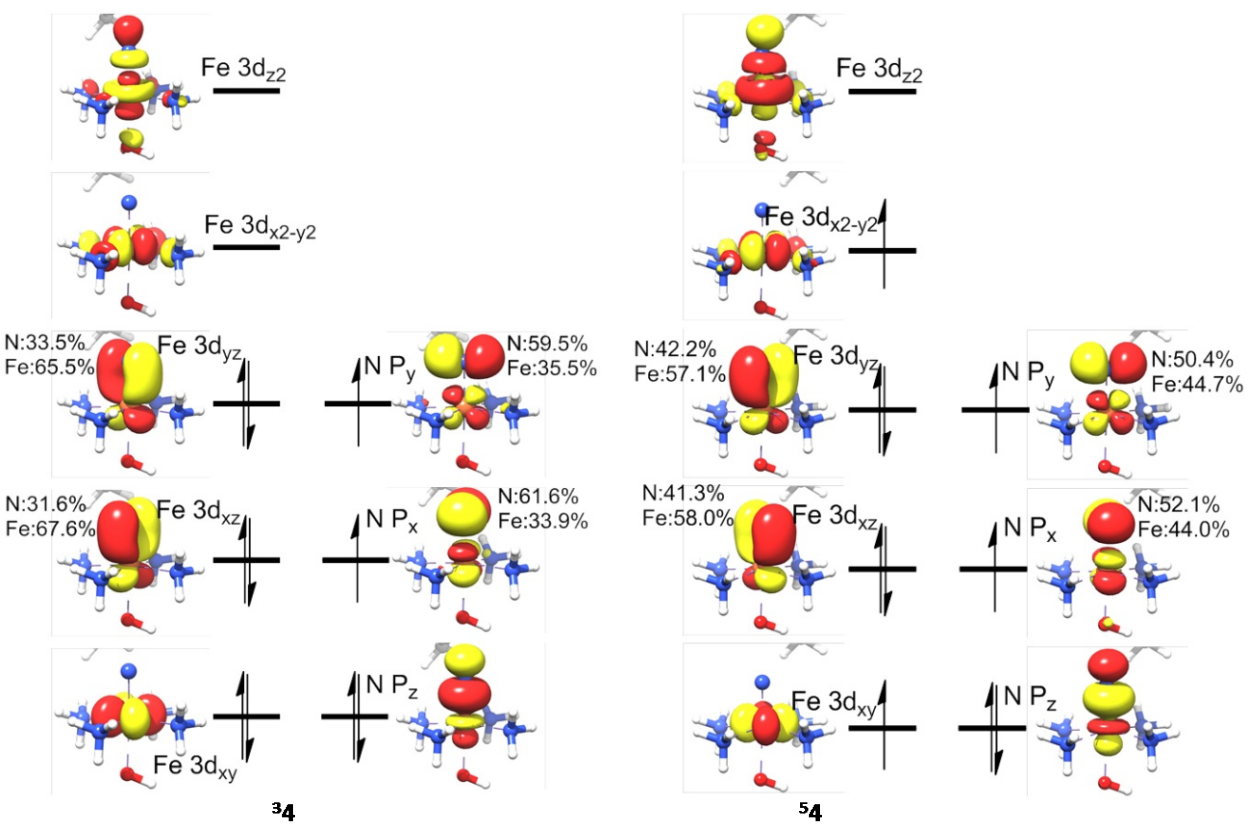
		Energy		Fe=E(E=O or N)	
		B3LYP	BP86	B3LYP	BP86
1	<sup>3</sup> 1	0.0	0.0	1.64	1.69
	<sup>5</sup> 1	3.6	2.5	1.64	1.68
2	<sup>2</sup> 2( <sup>2</sup> 2')	0.0(2.8)	0.0	1.72(1.65)	1.62
	<sup>4</sup> 2( <sup>4</sup> 2')	5.0(14.8)	6.7	1.68(1.75)	1.69
3	<sup>1</sup> 3	0.0	0.0	1.53	1.55
4	<sup>3</sup> 4	6.3	0.0	1.72	1.71
	<sup>5</sup> 4	0.0	3.8	1.69	1.70
5	<sup>2</sup> 5	0.0	0.0	1.70	1.62
	<sup>4</sup> 5	13.0	27.9	1.90	1.81
6	<sup>1</sup> 6	0.0	0.0	1.51	1.54

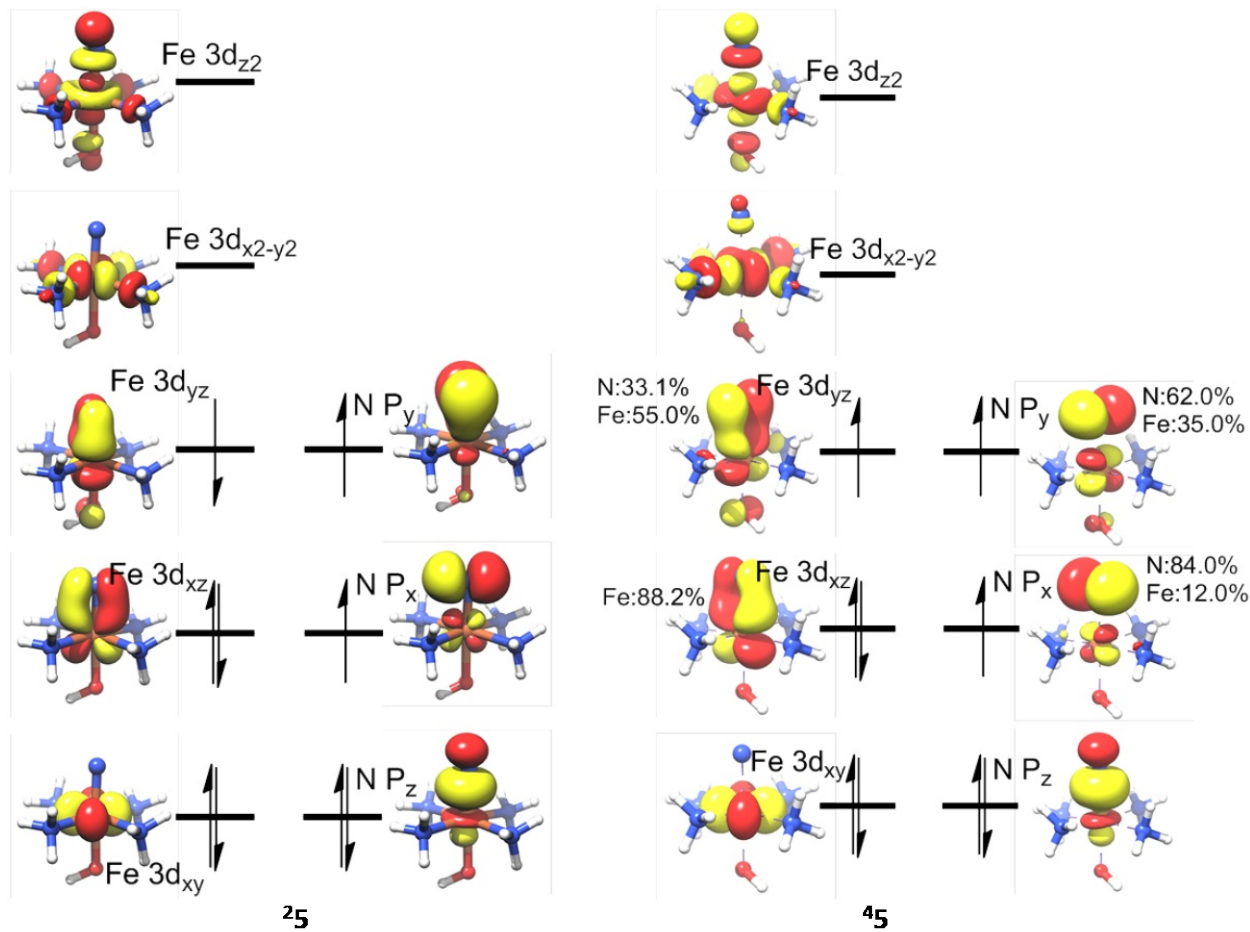












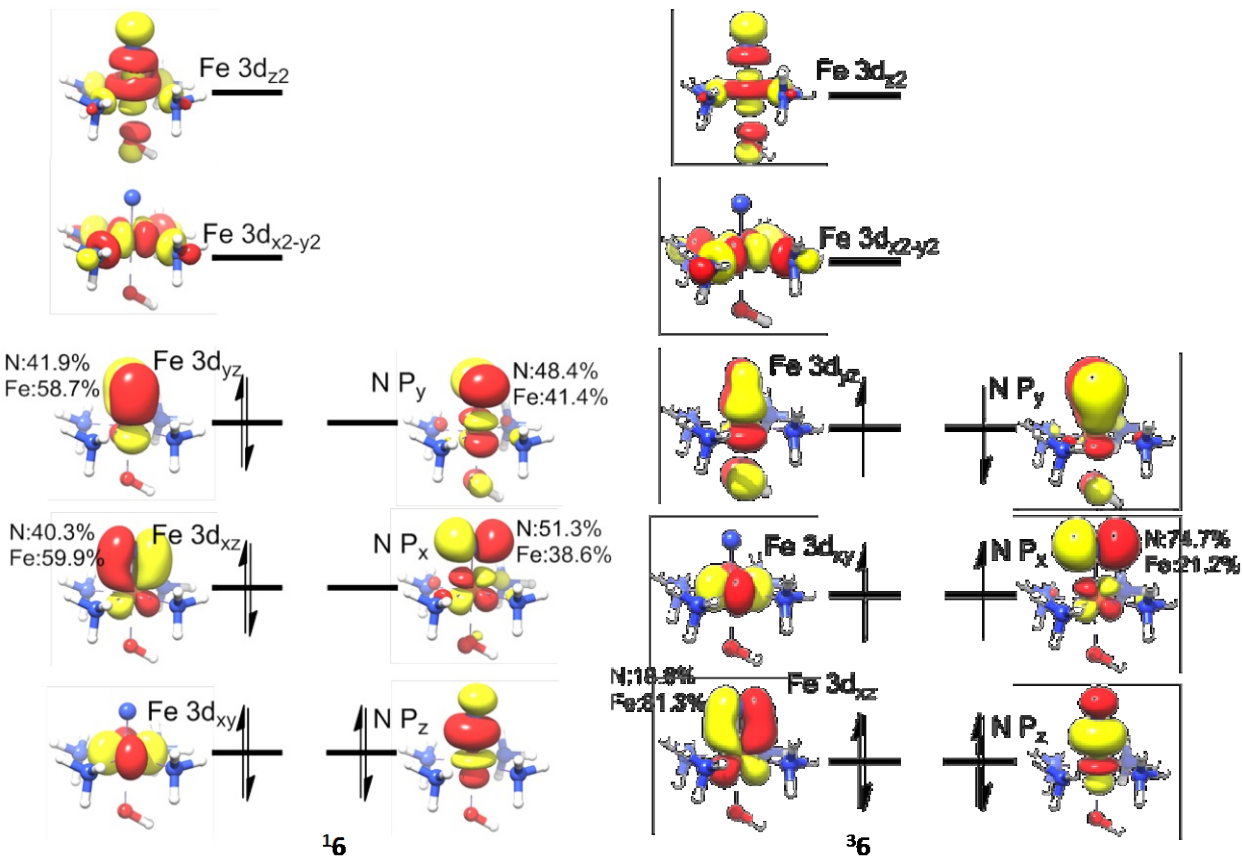
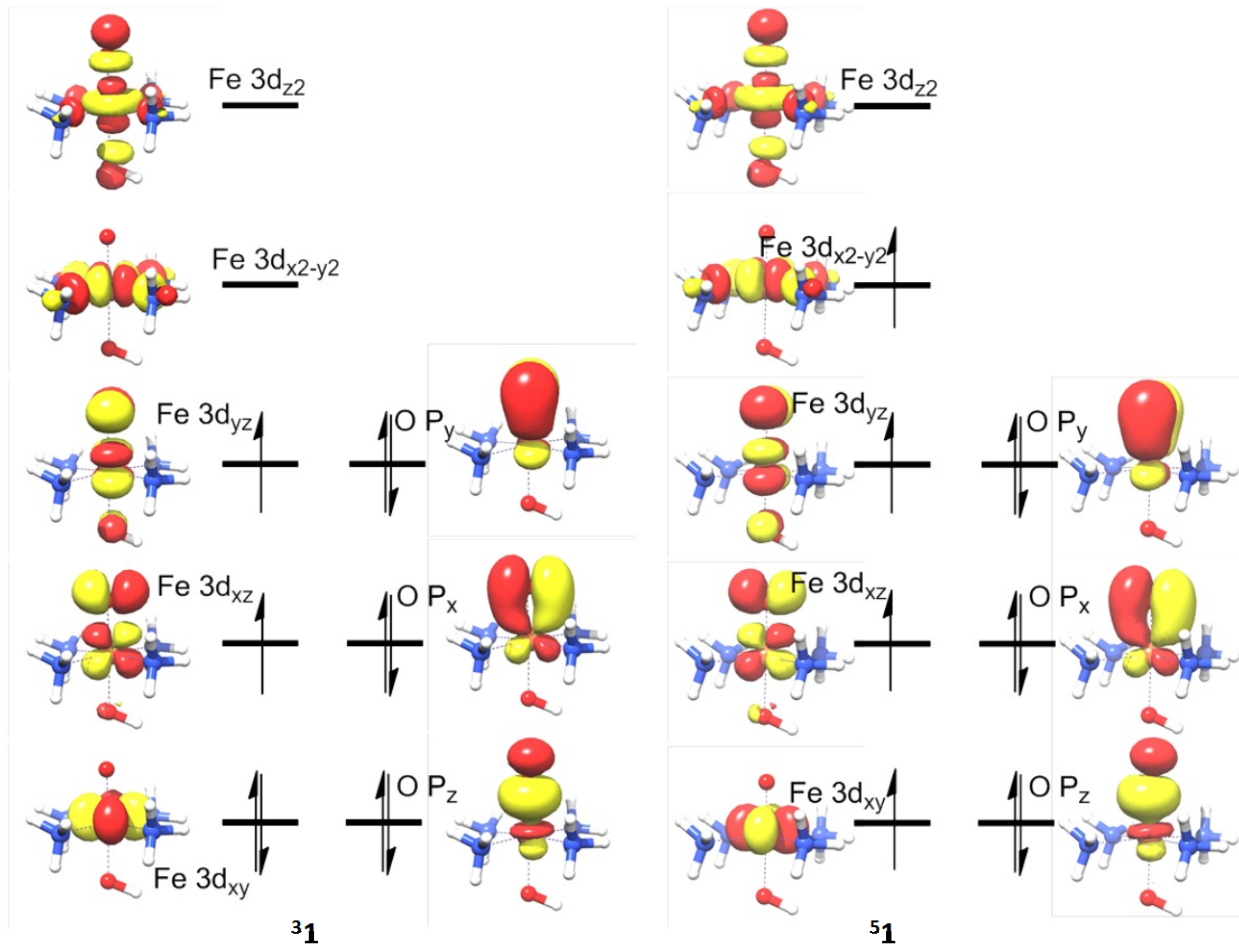
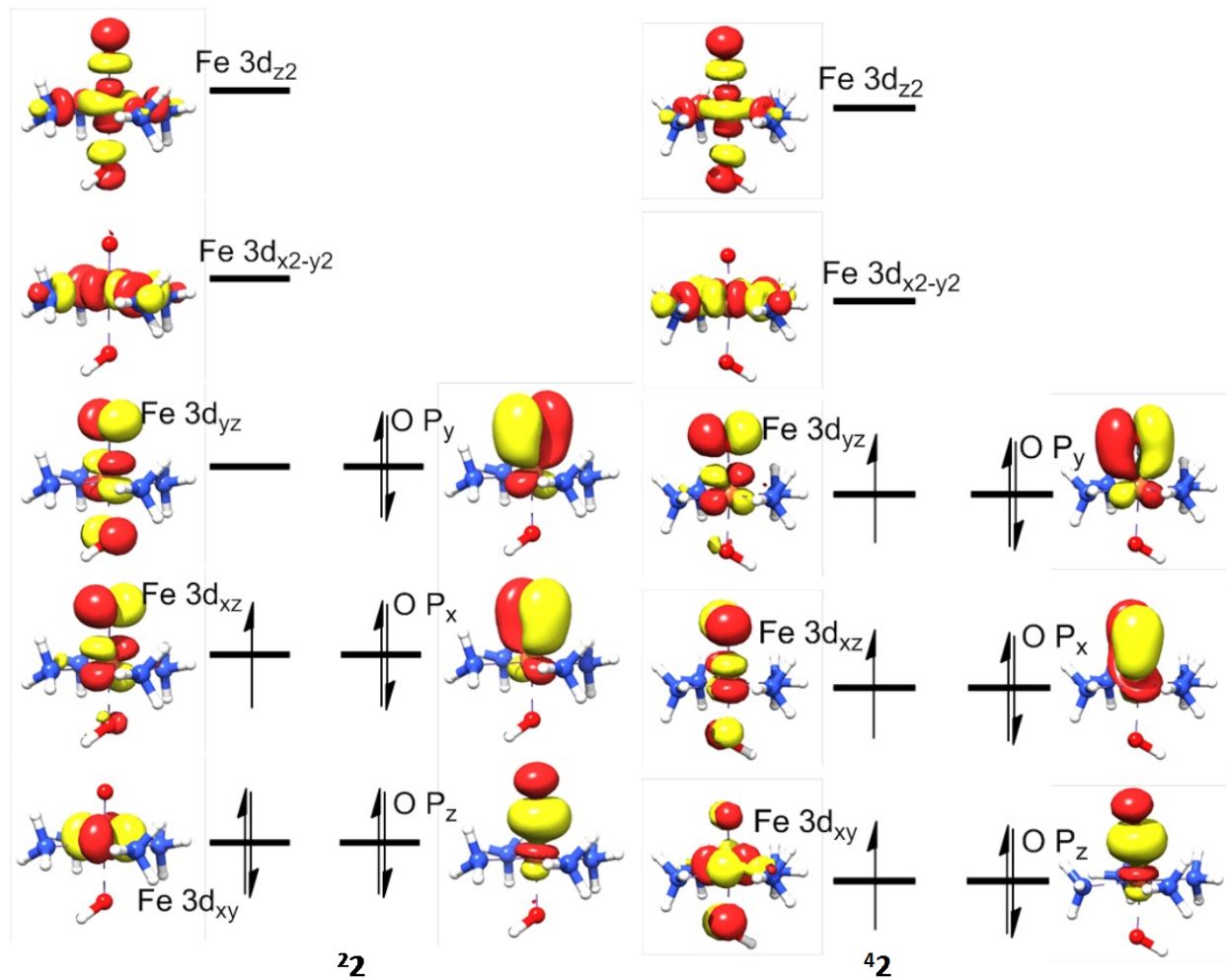
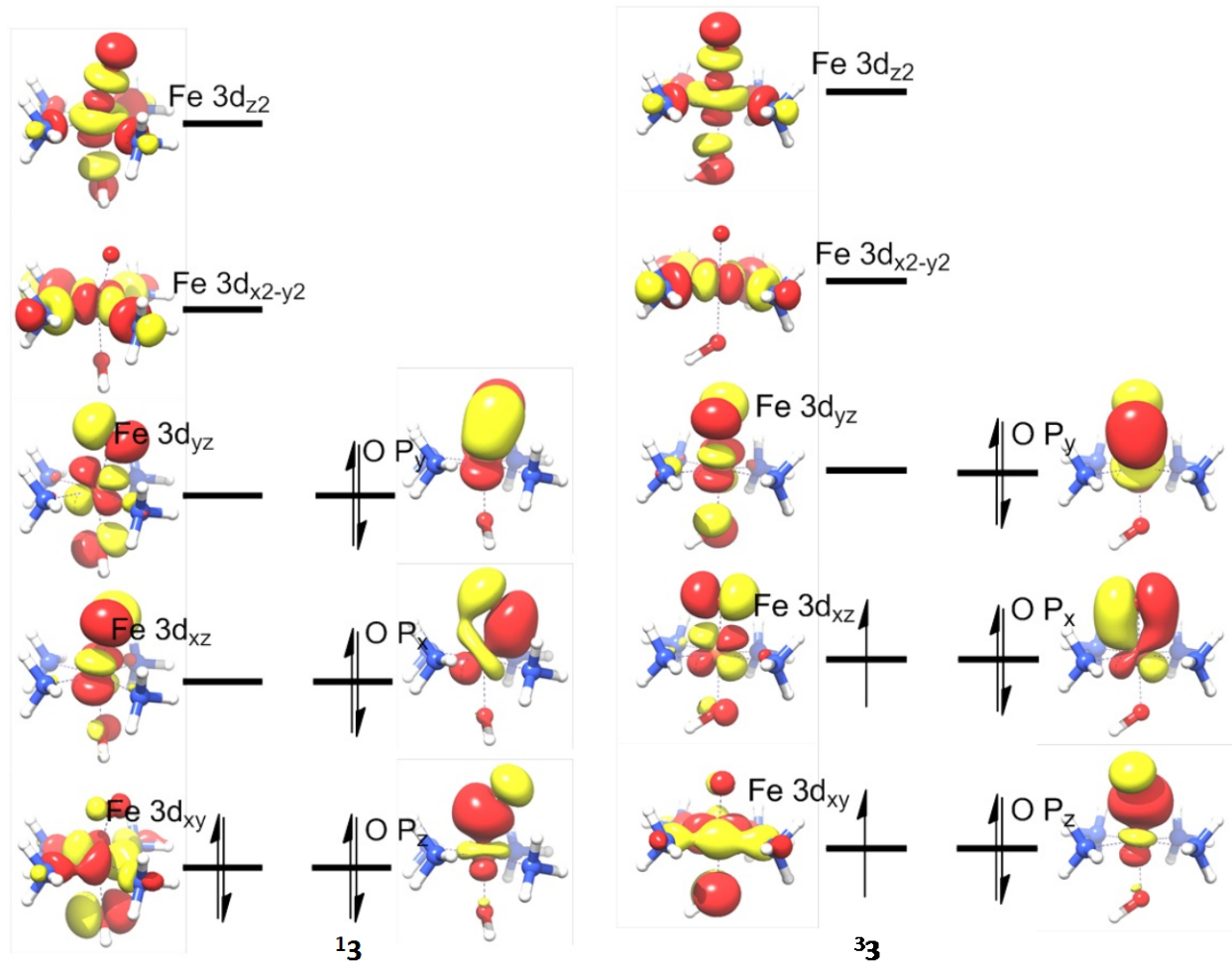
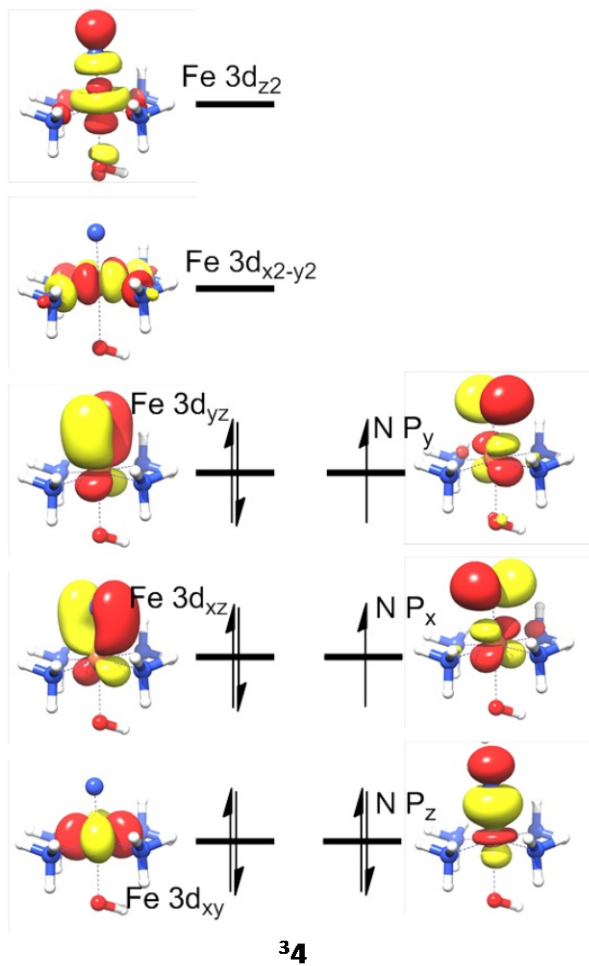


Figure S1. B3LYP Calculated Schematic MO diagrams for the “superoxidized” iron–oxo and –nitrido complexes.

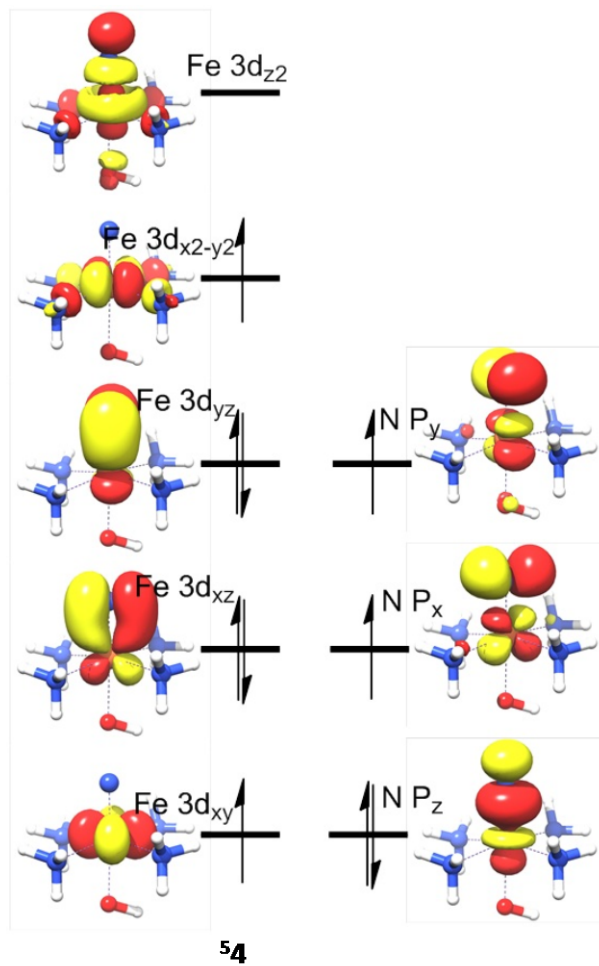




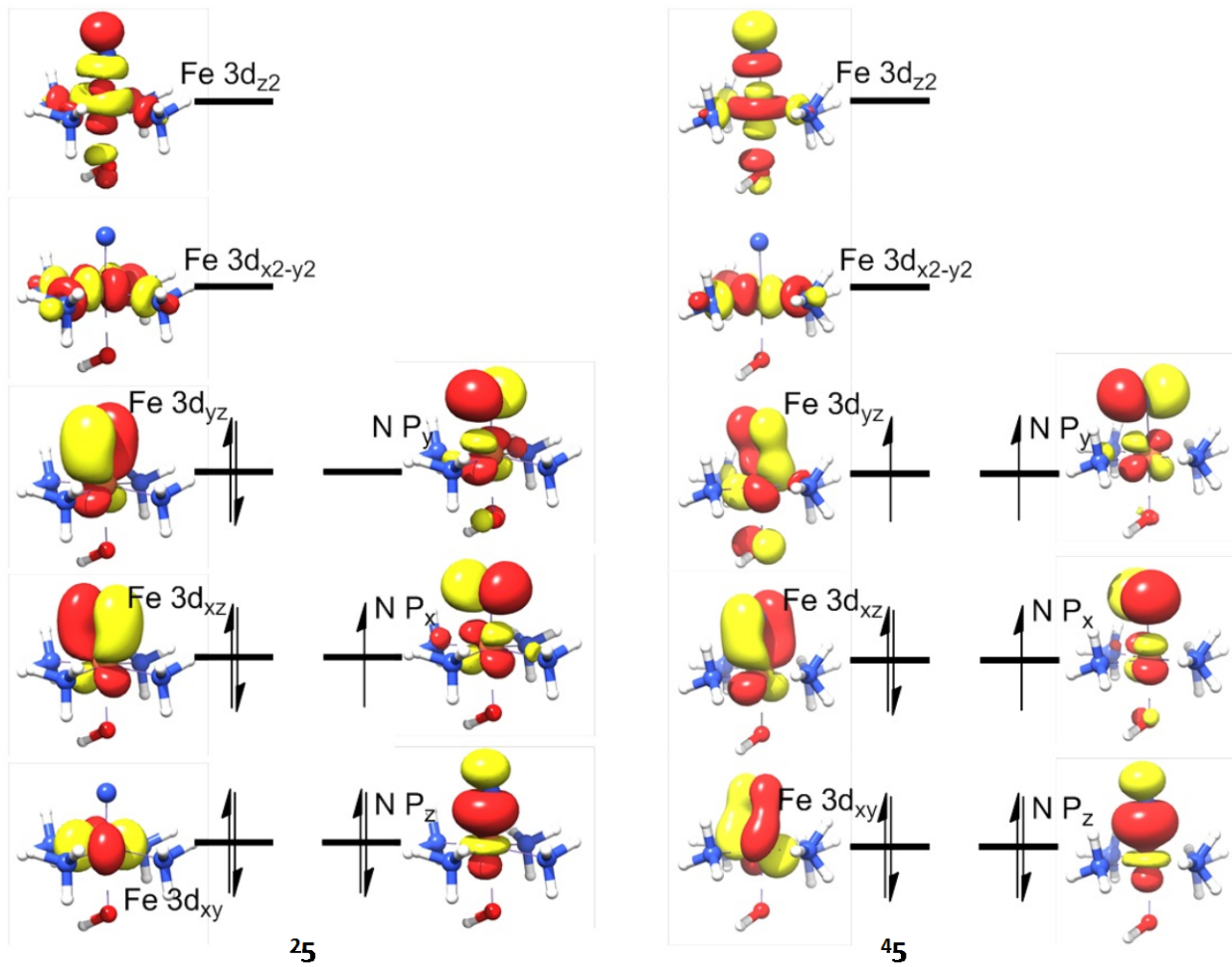




**3****4**



**5****4**



**25**

**45**

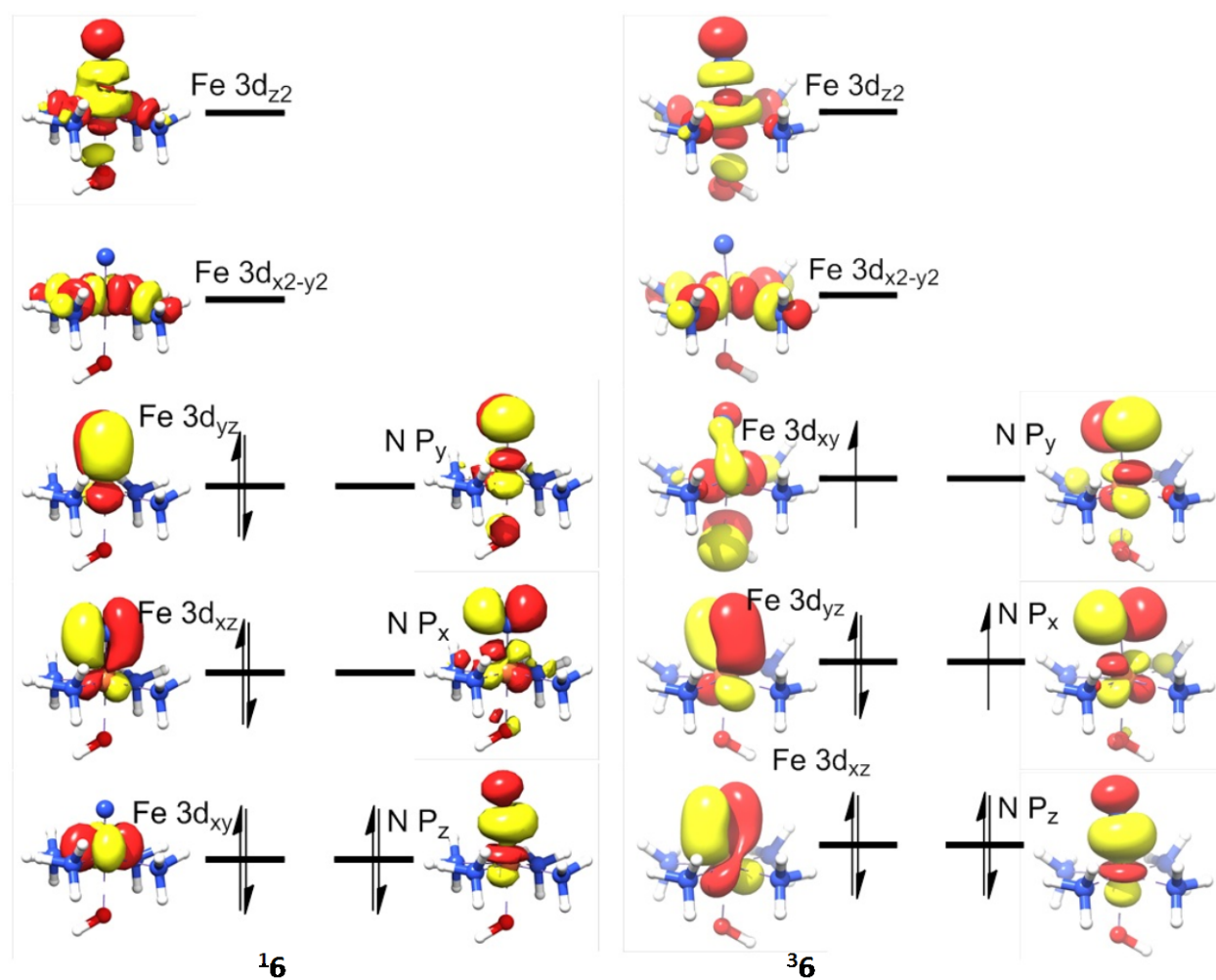
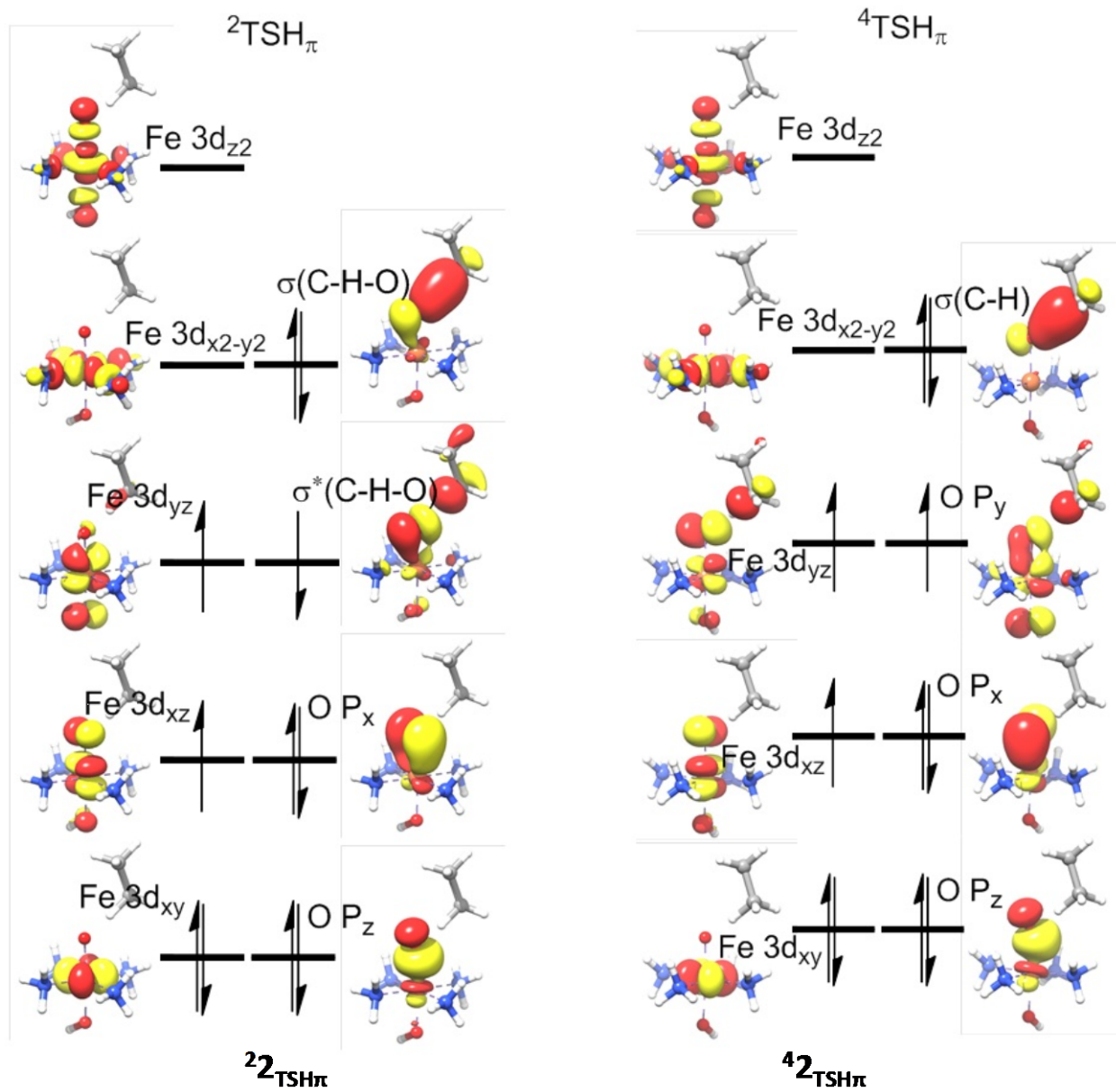
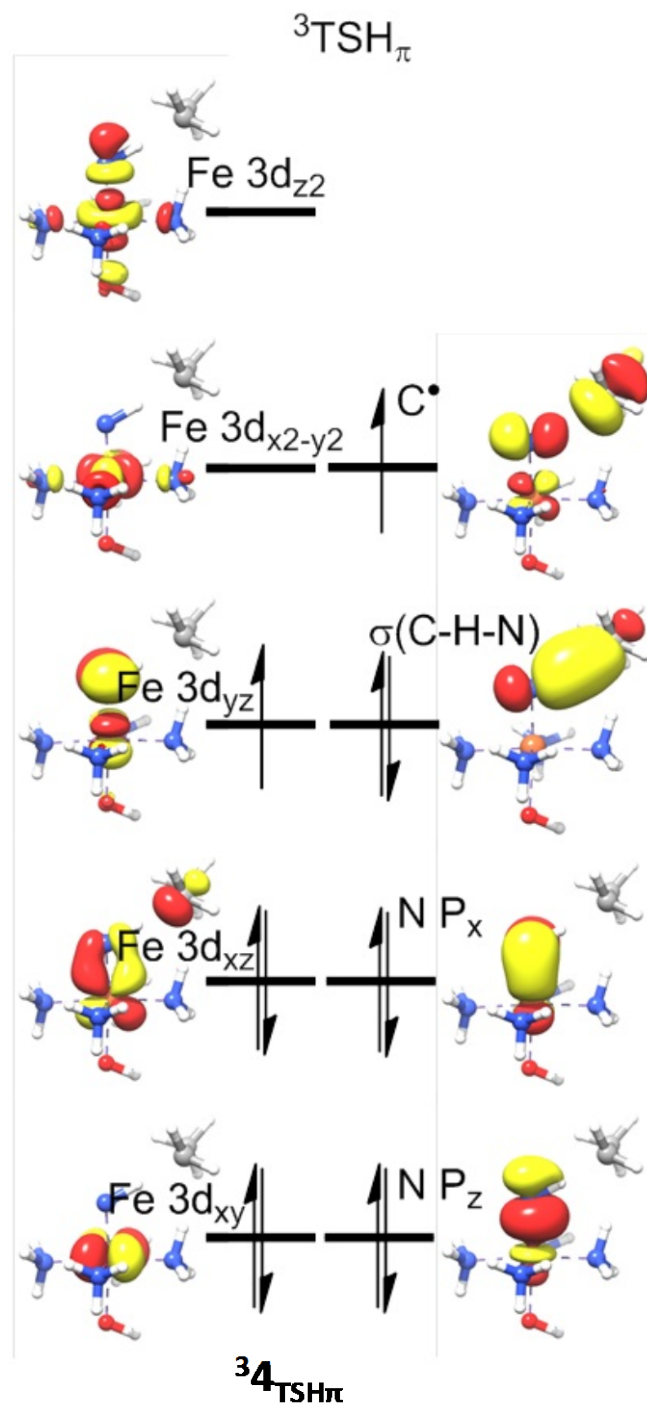


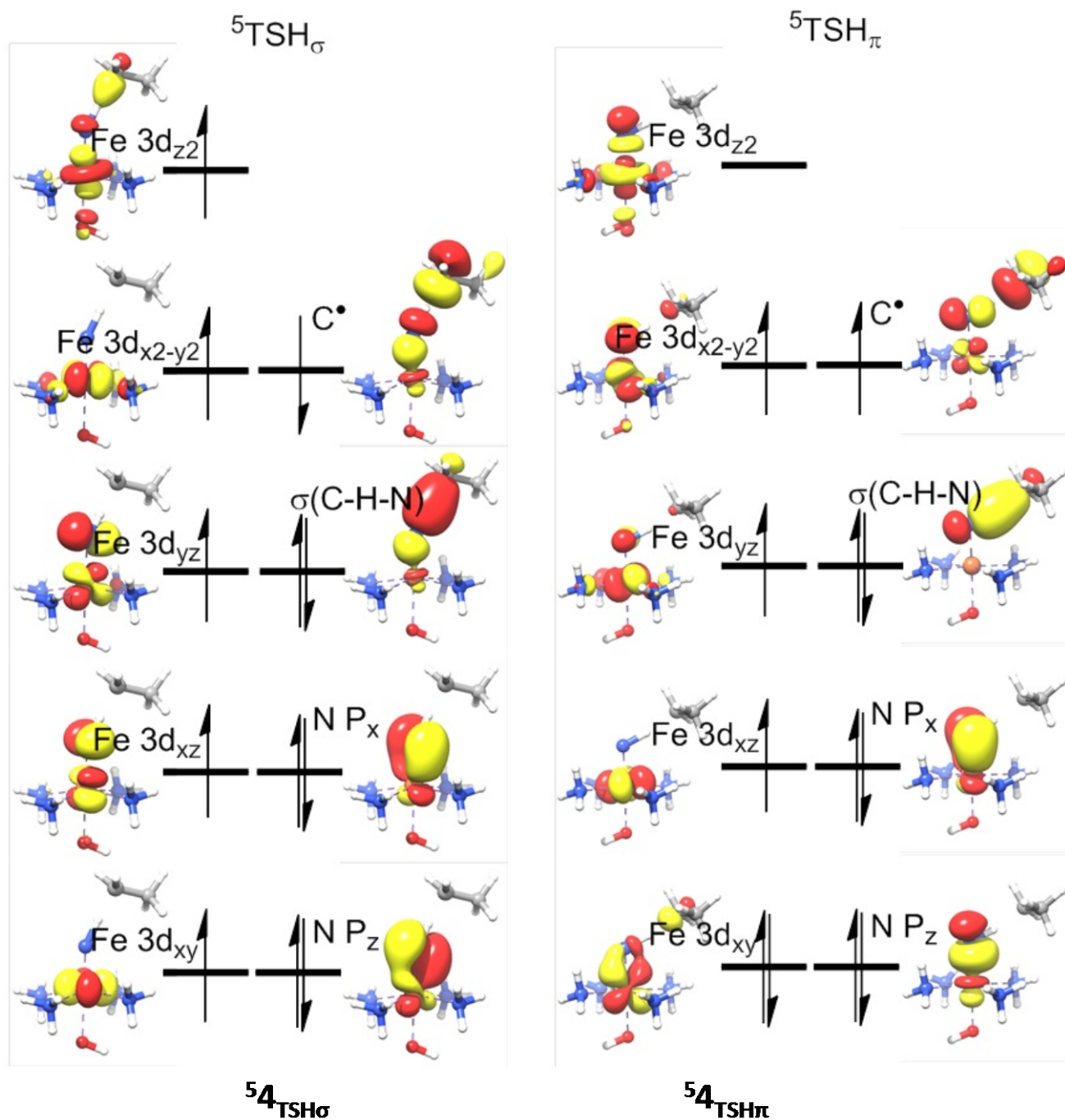
Figure S2. BP86 Calculated Schematic MO diagrams for the “superoxidized” iron–oxo and –nitrido complexes.

Table S2, B3LYP and BP86 Calculated Reaction Energies for All Iron-oxo and –nitrido oxidants.

	RC		$\Delta H^\ddagger$		$\Delta H$	
	B3LYP	BP86	B3LYP	BP86	B3LYP	BP86
<sup>3</sup> <b>1</b>	0.0	0.0	20.8	25.7	10.4	28.0
<sup>5</sup> <b>1<sub>σ</sub></b>	3.6	10.2	20.2	27.0	8.0	36.1
<sup>5</sup> <b>1<sub>π</sub></b>	3.6	10.2	22.7	38.7	12.7	35.0
<sup>2</sup> <b>2</b>	0.0	0.0	4.0	4.9	-7.0	3.1
<sup>4</sup> <b>2</b>	5.0	6.7	8.1	15.1	-5.6	5.7
<sup>1</sup> <b>3</b>	0.0	0.0	~	~	-20.2	4.0
<sup>3</sup> <b>4</b>	6.5	0.0	28.6	15.0	25.6	23.7
<sup>5</sup> <b>4<sub>σ</sub></b>	0.0	3.8	19.3	\	13.5	27.7
<sup>5</sup> <b>4<sub>π</sub></b>	0.0	3.8	25.2	19.1	9.0	13.0
<sup>2</sup> <b>5</b>	0.0	0.0	21.1	26.3	18.8	26.9
<sup>4</sup> <b>5</b>	130.	27.9	26.9	37.0	15.7	26.9
<sup>1</sup> <b>6</b>	0.0	0.0	~	~	16.7	31.4







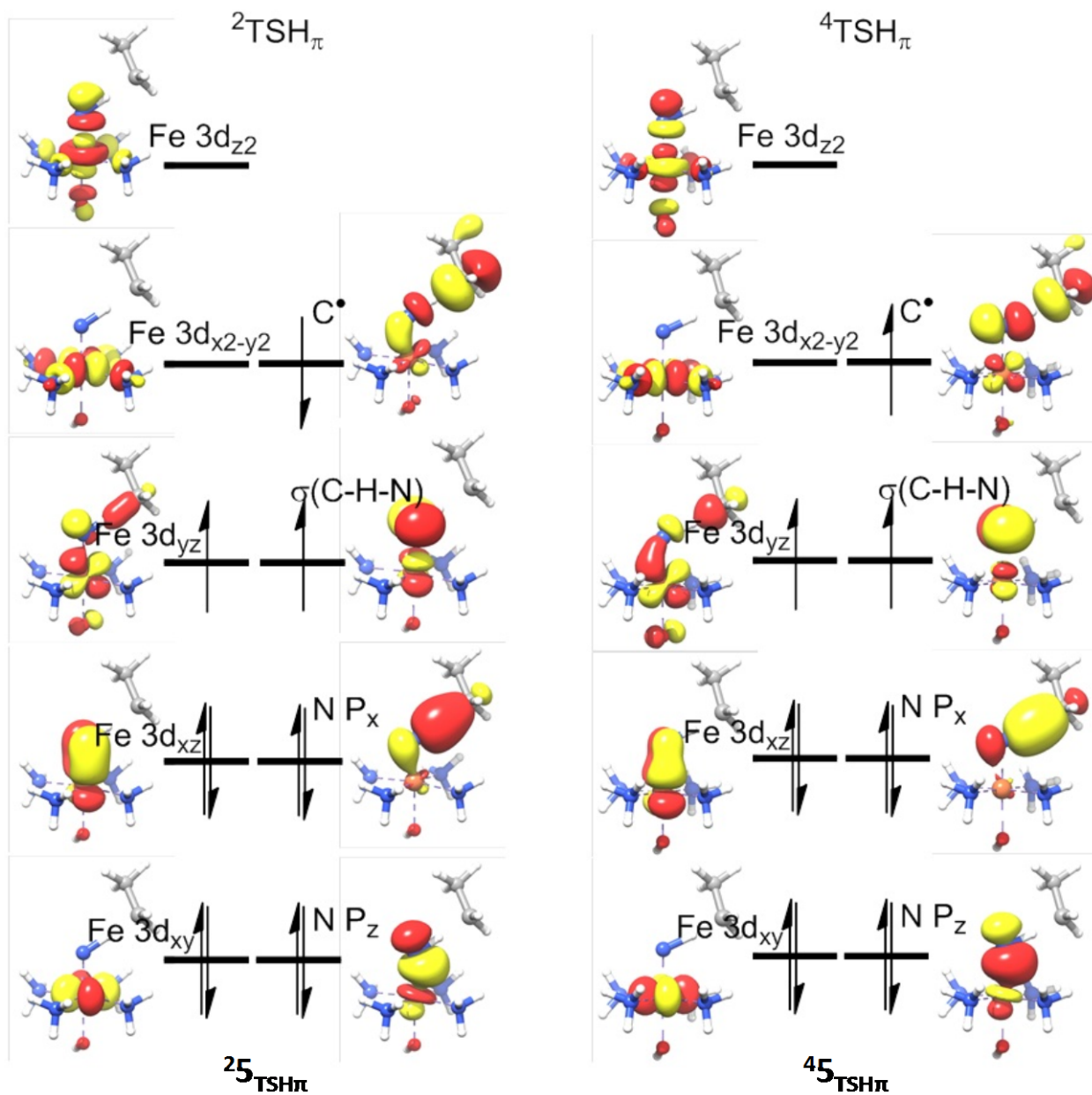


Figure S5. B3LYP Calculated Schematic MO diagrams for the transition states.

Table S3, Selected Key Geometric Parameters of Transition States for C-H Bond Activation by the “superoxidized” Iron Oxo and Nitrido Complexes (Bond Distances in Angstrom, Angles in Degree).

		Fe=E(E=O or N)		C-H		$\angle$ FeOH	
		B3LYP	BP	B3LYP	BP	B3LYP	BP
1	$^3\mathbf{1}_{\text{TSH}\pi}$	1.78	1.82 <sup>a</sup>	1.18	1.05 <sup>a</sup>	1.35	1.71 <sup>a</sup>
	$^5\mathbf{1}_{\text{TSH}\sigma}$	1.80	1.84 <sup>a</sup>	1.24	1.05 <sup>a</sup>	1.28	1.63 <sup>a</sup>
	$^5\mathbf{1}_{\text{TSH}\pi}$	1.80	1.82	1.19	1.05	1.35	1.72
2	$^2\mathbf{2}_{\text{TSH}\pi}$	1.73	1.70	1.47	1.30	1.18	1.26
	$^4\mathbf{2}_{\text{TSH}\pi}$	1.79	1.77	1.48	1.41	1.18	1.22
4	$^3\mathbf{4}_{\text{TSH}\pi}$	1.77	1.75	1.12	1.17	1.74	1.64
	$^5\mathbf{4}_{\text{TSH}\sigma}$	1.77	1.70 <sup>a</sup>	1.17	1.48 <sup>a</sup>	1.49	1.20 <sup>a</sup>
	$^5\mathbf{4}_{\text{TSH}\pi}$	1.77	1.75 <sup>a</sup>	1.13	1.12 <sup>a</sup>	1.65	1.80 <sup>a</sup>
5	$^2\mathbf{5}_{\text{TSH}\pi}$	1.72	~	1.16	~	1.51	~
	$^4\mathbf{5}_{\text{TSH}\pi}$	1.87	1.81	1.25	1.30	1.37	1.32
						118.7	115.8
						148.7	140.8
						119.9	117.1
						121.2	123.9
						122.0	125.2
						117.0	113.7
						155.8	167.4
						115.0	113.6
						122.2	~
						116.0	129.6

<sup>a</sup> get from scan calculation

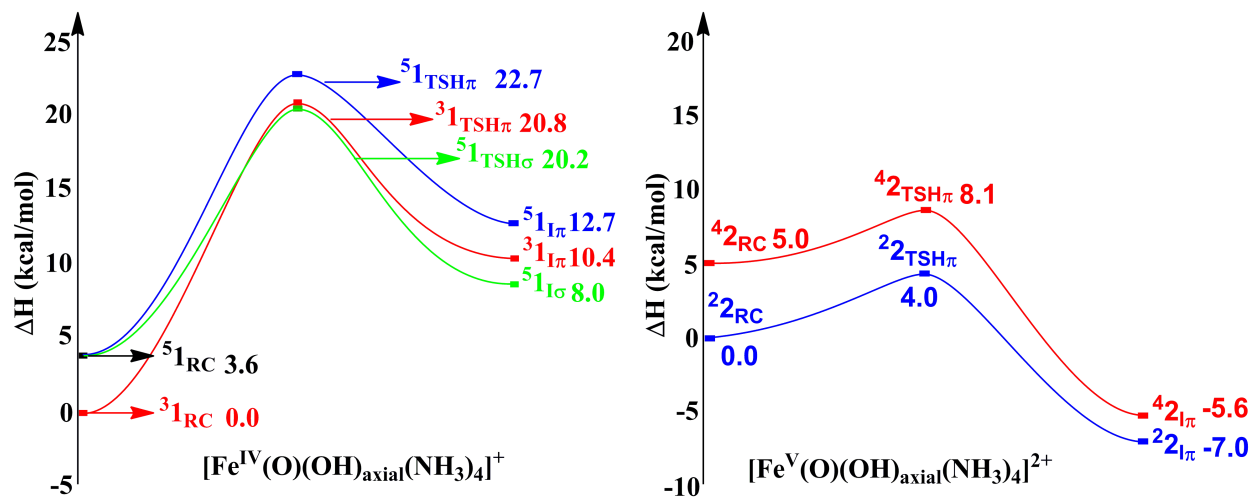


Figure S4. Schematic energy profiles ( $\Delta H$ ) for the ethane hydroxylation by complexes **1** ( $[\text{Fe}^{\text{IV}}\text{O}(\text{OH})(\text{NH}_3)_4]^+$ ) and **2** ( $[\text{Fe}^{\text{V}}\text{O}(\text{OH})(\text{NH}_3)_4]^{2+}$ ).

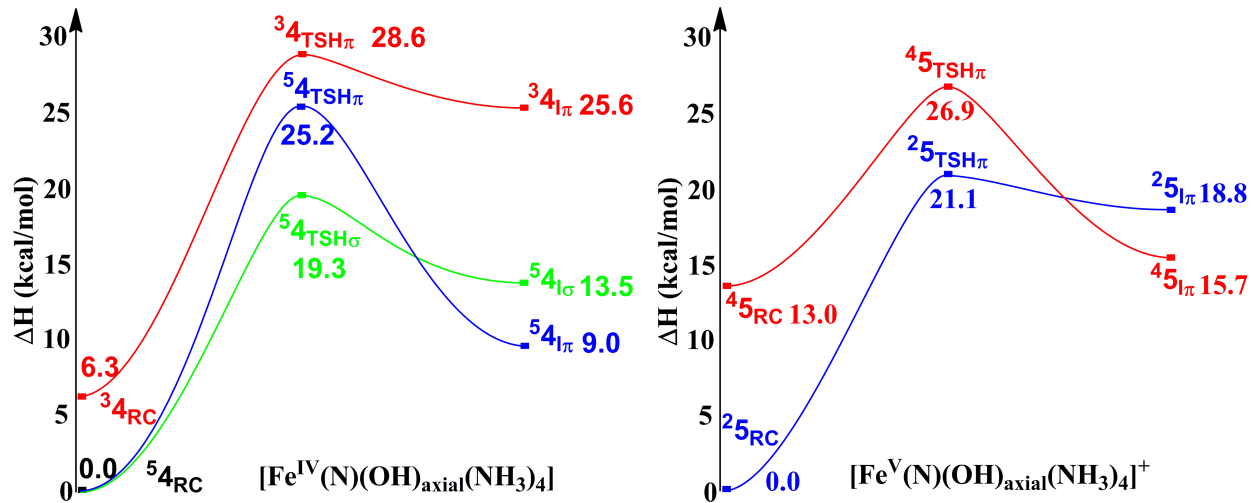


Figure S5. Schematic Gibbs free energy ( $\Delta G$ ) surfaces for the ethane C-H bond activation by the  $[\text{Fe}^{\text{IV}}\text{N}(\text{OH})(\text{NH}_3)_4]$  and  $[\text{Fe}^{\text{V}}\text{N}(\text{OH})(\text{NH}_3)_4]^+$  systems.

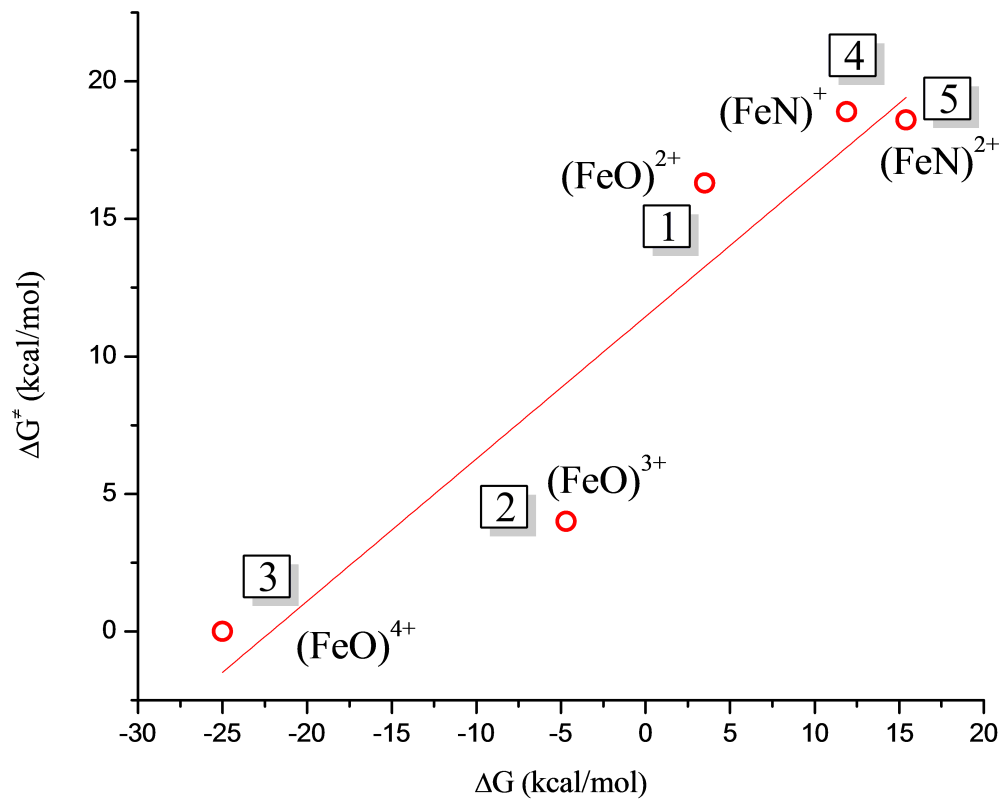


Figure S6. The activation barriers ( $\Delta G^\ddagger$ ) of **1 – 5** vs. the reaction free energies ( $\Delta G$ ).

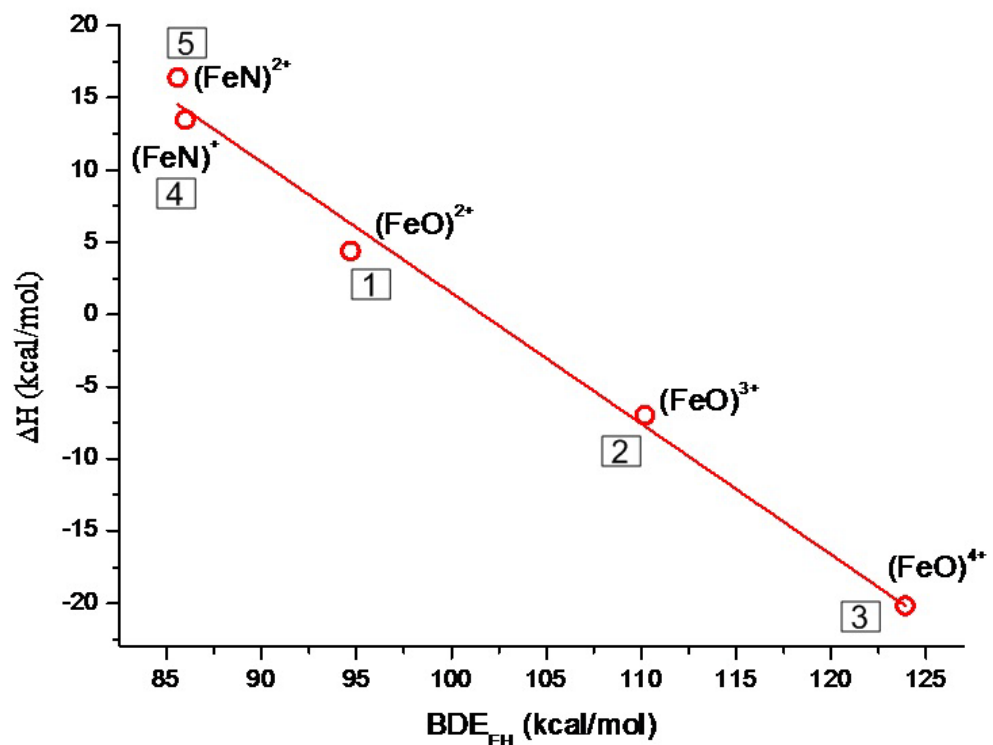


Figure S7. Reaction enthalpies vs.  $BDE_{E-H}$ .

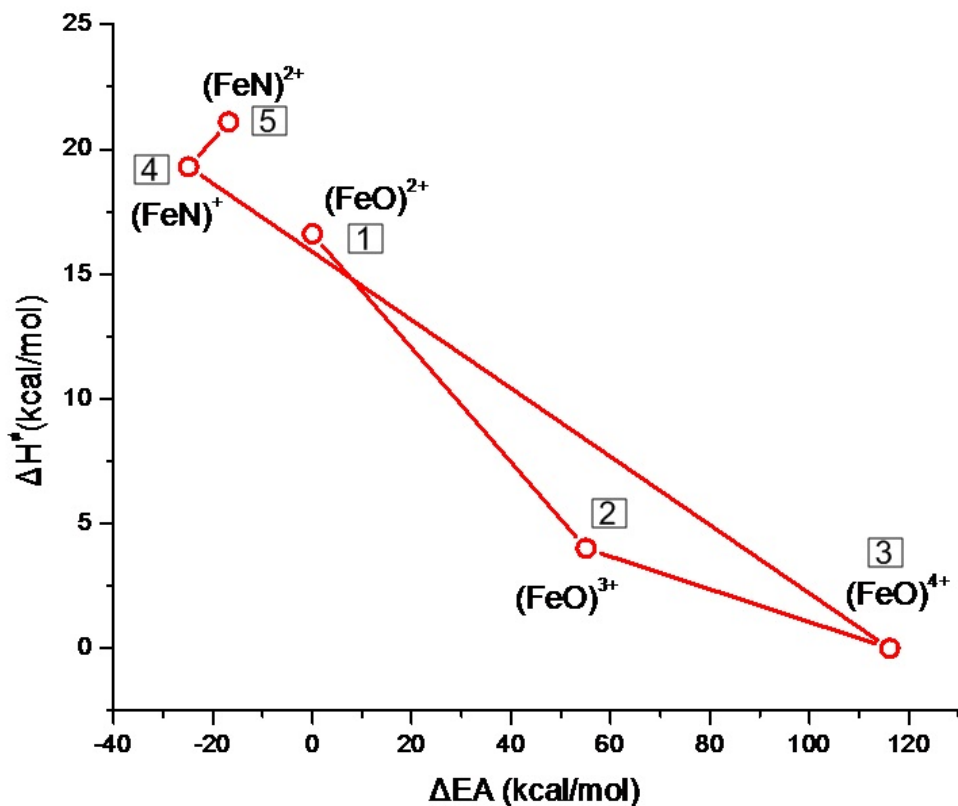


Figure S8. Reaction barriers vs. electron affinity (EA).